

JAAS

Accepted Manuscript



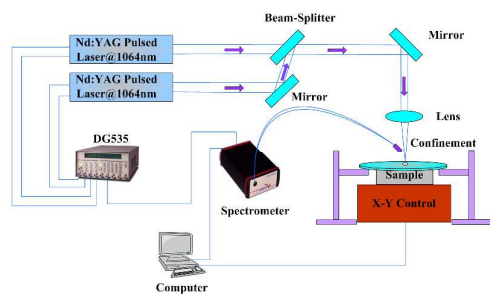
This is an *Accepted Manuscript*, which has been through the Royal Society of Chemistry peer review process and has been accepted for publication.

Accepted Manuscripts are published online shortly after acceptance, before technical editing, formatting and proof reading. Using this free service, authors can make their results available to the community, in citable form, before we publish the edited article. We will replace this *Accepted Manuscript* with the edited and formatted *Advance Article* as soon as it is available.

You can find more information about *Accepted Manuscripts* in the [Information for Authors](#).

Please note that technical editing may introduce minor changes to the text and/or graphics, which may alter content. The journal's standard [Terms & Conditions](#) and the [Ethical guidelines](#) still apply. In no event shall the Royal Society of Chemistry be held responsible for any errors or omissions in this *Accepted Manuscript* or any consequences arising from the use of any information it contains.

1
2
3 A cylindrical cavity is used to confine the plasma of collinear DP-LIBS, enhanced optical
4 emission with improved RSD and S/N ratio are achieved.
5



Optical emission character of collinear dual pulse laser plasma with cylindrical cavity confinement

Xuejiao Su Weidong Zhou* Huiguo Qian

Key laboratory of optical information detection and display technology of Zhejiang

Zhejiang Normal University, Jinhua, China 321004

Corresponding author: wdzhou@zjnu.cn

Abstract: Collinear dual pulse laser induced breakdown spectroscopy with and without cavity confinement were carried out on Si crystal sample by using two Nd: YAG laser sources emitting at 1064 nm and a 1 mm-height and 3 mm-diameter aluminum cylindrical cavity. Nearly 2-3 times enhanced optical emission intensity with a higher signal to noise ratio was observed when an additional cylindrical cavity was used to confine the laser plasma. The inter-pulse delay time to achieve the maximum atomic and ionic line intensity was optimized for both confined and unconfined collinear dual pulse laser plasma, and a modest difference of the optimized inter-pulse delay time was found. Based on the relative standard deviation of several selected Si line intensities, it was ascertained that the signal intensity from confined collinear dual laser plasma emission showed a better stability. Plasma temperature and electron number density of confined collinear dual pulse laser plasma had been measured and compared with that of unconfined laser plasma as well.

Keywords: Laser induced breakdown spectroscopy, Spatial confinement, Collinear dual pulse, Plasma enhancement

1 Introduction

In the last decade, laser-induced breakdown spectroscopy (LIBS)[1-3] was a very popular and rapid developed technique in the field of analytical atomic spectroscopy. This technique, allowing for rapid, multi-elemental analysis with very little or no sample preparation, has been proposed as an important tool for in site monitoring of trace pollutants in environment[4], as well as in a wide range of other analytical applications[5-8].

However, in compare with other spectroscopy methods, LIBS always suffers a relatively poor sensitivity and measurement uncertainty, which in turn restricts its further development and quantitative analytical application. To date, a number of methods have been proposed to improve the sensitivity and reduce the measurement uncertainty, including using dual pulse(DP) laser excitation[9-11], discharge enhancement[12-15], plasma confinement[16-20], *etc.* to reheat the laser plasma. Generally, these methods have successfully enhanced the optical emission intensity and to

1
2
3
4 some extend have improved the overall sensitivity of LIBS [8, 17, 21]. To further improve the LIBS
5
6 performance, the combinations of these methods mentioned above might be able to play a significant
7
8 role. For example, a crossing beam dual pulse (DP) LIBS has recently been combined with a pair of
9
10 aluminum-plate away from 11mm to spatially confine the cross beam dual pulse laser plasmas from
11
12 two sides[22], a significant enhancement of emission intensity of the Cr lines was observed comparing
13
14 to that in crossing beam DP-LIBS. Like crossing beam dual pulse LIBS technique, collinear dual pulse
15
16 LIBS is also an important and wide used technique to enhance laser plasma emission in our LIBS
17
18 society. Therefore, to further improve the collinear dual pulse LIBS performance and to know how the
19
20 combination of collinear dual pulse with a cavity will affect the laser plasma emission is interesting.
21
22 However, no directed study has been performed so far on the combination effect of collinear dual pulse
23
24 excitation with a cavity confinement.

25
26
27 In this article, an experimental configuration, two collinear pulse laser beams and a cylindrical cavity
28
29 are combined together to generate and confined laser plasma, and are used to evaluate the performance
30
31 of the confined collinear dual pulse LIBS. The optical emission characters of the confined plasmas, as
32
33 well as the temperature and electron number density of the plasma were carefully investigated.

34 35 **2 Experimental**

36
37
38 A schematic diagram of the experimental setup is shown in Figure 1. The laser system consists of
39
40 two identical Nd : YAG lasers, both operated at wavelength 1064 nm with a repetition rate of 1 Hz and
41
42 a pulse width of 10 ns. The laser energy can be adjusted continuously from 0 to 180 mJ, depending on
43
44 the experimental requirements. The inter-pulse delay time Δt between two laser pulses and the data
45
46 acquisition delay time t_d of the spectrometer after the first laser pulse were controlled by a digital pulse
47
48 delay generator (Model DG535, Stanford Instruments).

49
50
51 All the experiments were carried on under the normal atmospheric condition. In the collinear
52
53 dual-pulse LIBS experiments, the two laser beams were carefully adjusted to a co-axes configuration.
54
55 The beam propagation directions were perpendicular to the sample surface. During all the data
56
57 acquisition processes, the total energy of two laser beams was set to be 40 mJ, and the energy of each
58
59 laser beam was set to be equal (20 mJ / pulse, *i.e.* total energy $E = 20 \text{ mJ} + 20 \text{ mJ}$). The lasers were
60
focused on the surface of Si crystal by a convex lens of 70 mm focal length, and the lens to sample

1
2
3
4 distance was set to be 1 mm less than the focal length, in order to avoid the air breakdown in front of
5
6 the target and to improve the stability of the plasma. The Si crystal sample was mounted on a
7
8 motorized X-Y translation stage in order to ablate a fresh spot at each dual-pulse-laser excitation and to
9
10 avoid over ablation. In the cylindrical cavity confined experiments, a 3 mm diameter cylindrical hole
11
12 was drilled in an aluminum plate of 1 mm thickness. Two height-adjustable poles were used to hold the
13
14 aluminum plate. So the aluminum plate can be placed near the sample surface but about 100 μm higher
15
16 than the sample surface, and be able to avoid movement during the translation of the sample. Two
17
18 collinear laser beams hit the sample through the center of the hole, and the laser plasma plumes were
19
20 produced at the center of the cylindrical cavity.

21
22 The optical emission from the plasma was collected by using a collimating lens at an angle of 30° to the
23
24 laser beam. A bundle of 200 μm -diameter, multimode optical fibers with SMA connector was used to
25
26 deliver the collected light to an Avaspec-2048 fiber optic Spectrometer. The spectrometer provided an
27
28 average spectral resolution of ~ 0.1 nm (FWHM) in a broad continuous spectral range between 196 to
29
30 500 nm. The detector was a CCD linear array having 2048 pixels, which can be externally triggered to
31
32 start signal integration with an integrating time of 2 ms. Software was used to read the data from the
33
34 chip and also to build the spectrum. This made it possible to measure a large wavelength range (196 ~
35
36 500 nm) simultaneously. In order to increase the signal-to-noise ratio (S/N) and improve the precision
37
38 of the measures, for each experiment, 100 spectra had been collected, and all the spectra presented here
39
40 were the averaged spectra of 20 accumulations. Such an averaged spectrum was then served as one
41
42 measurement, and so 5 such independent replicate measurements were carried out for each experiment
43
44 and were used for deriving the relative standard deviation (RSD) of the measured line peak intensity.

45
46 In all the calculations of S / N ratio, as Nassef et al. reported in reference[12], the background value
47
48 was determined by taking the average value of continuing 10 data points where there was no detectable
49
50 spectral line, and all the 10 data points were selected near each interested spectral line. After
51
52 background subtraction, the line intensity was then obtained, and the standard deviation of the values of
53
54 10 data points was used as the noise level for calculation of the S/N ratio of the interested spectral line.
55
56
57
58
59
60

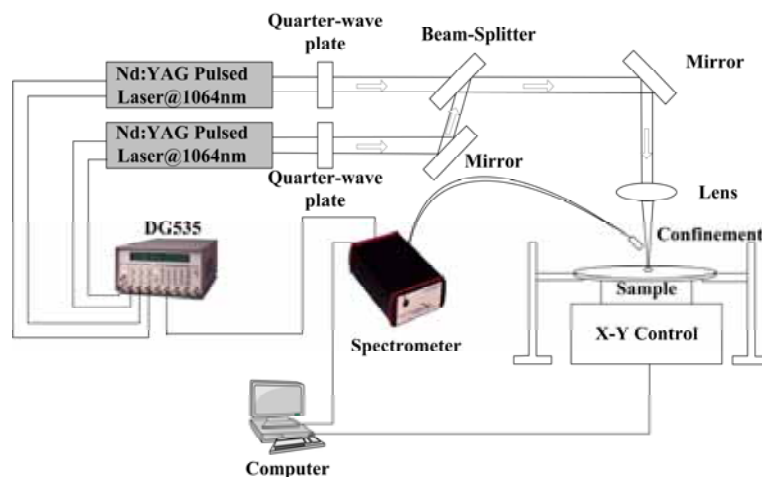


Figure 1. Schematic diagram of the experimental setup

3. Results and discussion

3.1. Emission spectra

The typical spectra of collinear DP-LIBS and collinear DP-LIBS combined with cylindrical cavity confinement were measured at total laser energy of 40 mJ as stated above. For clarification, only the expanded spectra of a small wavelength range are shown Figure 2. The S/N ratio and relative standard deviation (RSD) of the atomic lines Si I 212.41 nm, Si I 221.67 nm, Si I 243.52 nm, Si I 263.13 nm, and the ionic lines Si II 207.20 nm, Si II 235.63 nm are calculated and shown in Figure 2 as well. The optical emission of the confined collinear dual pulse laser excited plasma is indeed characterized by a higher intensity, better signal to noise ratio (S/N) and improved stability in terms of relative standard deviation compare with the corresponding plasma emission generated by dual pulse excitation. The signal intensity enhancement phenomenon is actually similar to that observed in confined single pulse laser excitation either caused by laser craters[23] or by various shapes of confinement cavity[16, 18, 19, 23]. And it had also been observed in a cross beam dual pulse laser excitation with a pair of plates confinement[22]. The main mechanism of this intensity enhancement phenomenon is that the formation and expansion of laser induced plasma in gas circumstance is accompanied by the formation of a shock wave. As a result, if a small obstacle is placed across a shock wave path, the wave will be back reflected to the plasma front by the obstacle. This back reflection leads to an increase of the number of collisions among particles in the plasma, which in turn results in an increase of the number of atoms and ions in high-energy states and so an enhancement of emission intensity[16, 19, 23, 24]. Several selected Si atomic and ionic line intensities are listed in the table 1, together with the relative standard deviation (RSD) of five replicate measurements. The enhance factor, which is defined as the peak

intensity ratio of the confined DP-LIBS signal to the corresponding unconfined DP-LIBS signal with the same laser ablation energies and delay time are also listed in table 1, Typically, 2 - 3 times signal enhancements were observed for most of the Si lines in the collinear DP-LIBS spectrum with cylindrical cavity confinement.

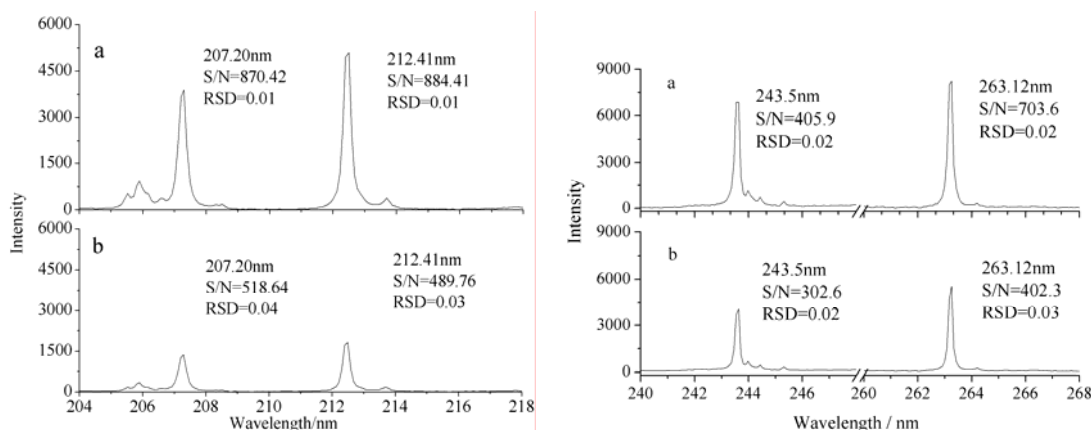


Figure 2 Typical spectra of DP-LIBS with (a) confinement and (b) without confinement, Both spectra were recorded at laser energy 40mJ ($E = 20\text{mJ} + 20\text{mJ}$, $\Delta t = 1.5 \mu\text{s}$, $t_d = 1.0 \mu\text{s}$)

Table 1. The enhancement of line intensity and S/N ratio of Si lines ($E = 20\text{mJ} + 20\text{mJ}$, $\Delta t = 1.5 \mu\text{s}$, $t_d = 1.0 \mu\text{s}$)

Wavelength (nm)	Intensity		RSD			
	without cavity	with cavity	Enhance Factor	without cavity	With cavity	Improve Factor
Si I 212.41	1817.15	5093.81	2.8	0.03	0.01	3
Si I 221.67	1429.72	3777.47	2.6	0.06	0.03	2
Si I 243.52	4052.89	6877.46	1.7	0.02	0.02	1
Si I 263.13	5540.15	8246.08	1.5	0.03	0.02	1.5
Si II 207.20	1366.91	3894.40	2.9	0.04	0.01	4
Si II 235.63	1087.38	1756.77	1.6	0.11	0.07	1.6

Similar to that using spatial confinement in single pulse LIBS, the spatial confined DP-LIBS will lead to more atoms and ions been excited to upper electronic states, and so the optical emission was enhanced. Furthermore, this intensity enhancement is dependent on the inter-pulse delay time as well. In Figure 3, the time integrated line intensity versus inter-pulse delay time between two pulse lasers is shown for selected Si I and Si II transitions in both the confined and unconfined dual pulse laser excitation. For the given laser energy and gate delay time, the emission of all selected Si atomic and ionic lines increased sharply at a short inter-pulse delay time and then gradually decreased at longer delay time within the measured delay time range up to $\sim 9 \mu\text{s}$. For the confined dual pulse laser

1
2
3
4 excitation, the best signal intensity for atomic and ionic spectral lines can be obtained with the
5
6 inter-pulse delay time $\sim 1.2 \mu\text{s}$. Moreover, at the optimized delay time, the Si 207.20 nm line intensity
7
8 of the confined laser plasma was about 2.9 times higher than that without a cavity confinement. But for
9
10 unconfined dual pulse LIBS, the best inter-pulse delay time for the observed maximum signal intensity
11
12 are shorter than that in confined dual pulse LIBS, which are about $1.0 \mu\text{s}$ for atomic lines and $1.5 \mu\text{s}$ for
13
14 ionic lines, respectively. Indicating the plasma confinement not only will enhance the plasma emission,
15
16 it also will affect the inter-pulse time delay to achieve the best performance in the collinear dual pulse
17
18 LIBS. A plasma emission enhancement by collinear DP-LIBS is mainly attributed to the plasma
19
20 reheating by the second laser[9-11]. Therefore the morphology of plasma plume and particle density in
21
22 the interacting region of the first laser plasma with the second laser beam will greatly affect the overall
23
24 particles been reheated by the second laser, and hence affect the enhancement. As indicated in the early
25
26 section of this article and in other reports [16-20, 24], the plasma emission enhancement by the cavity
27
28 is actually due to the compression of the plasma plume by the reflected shock wave. And the plasma
29
30 plume compression will affect the temporal morphology of plasma[25] as well as the time dependent
31
32 particle number density in the interaction region[20]. Therefore there will have a different delay time to
33
34 achieve the best performance in collinear DP-LIBS with and without the cavity confinement.

35
36 Except for the enhancement of line intensity, the signal to noise (S/N) ratio has also significantly
37
38 improved in the confined dual pulse LIBS spectra. For example, the S/N ratio of atomic line Si I 212.41
39
40 nm was 489.76 in unconfined collinear DP-LIBS, while the value increased to 884.41 in confined
41
42 collinear DP-LIBS. The S/N ratio of ionic line has improved as well, it gave a value of 870.42 for Si II
43
44 207.20 nm line in confined collinear DP-LIBS, while the value was 518.64 in unconfined collinear
45
46 DP-LIBS.
47
48
49
50
51
52
53
54
55
56
57
58
59
60

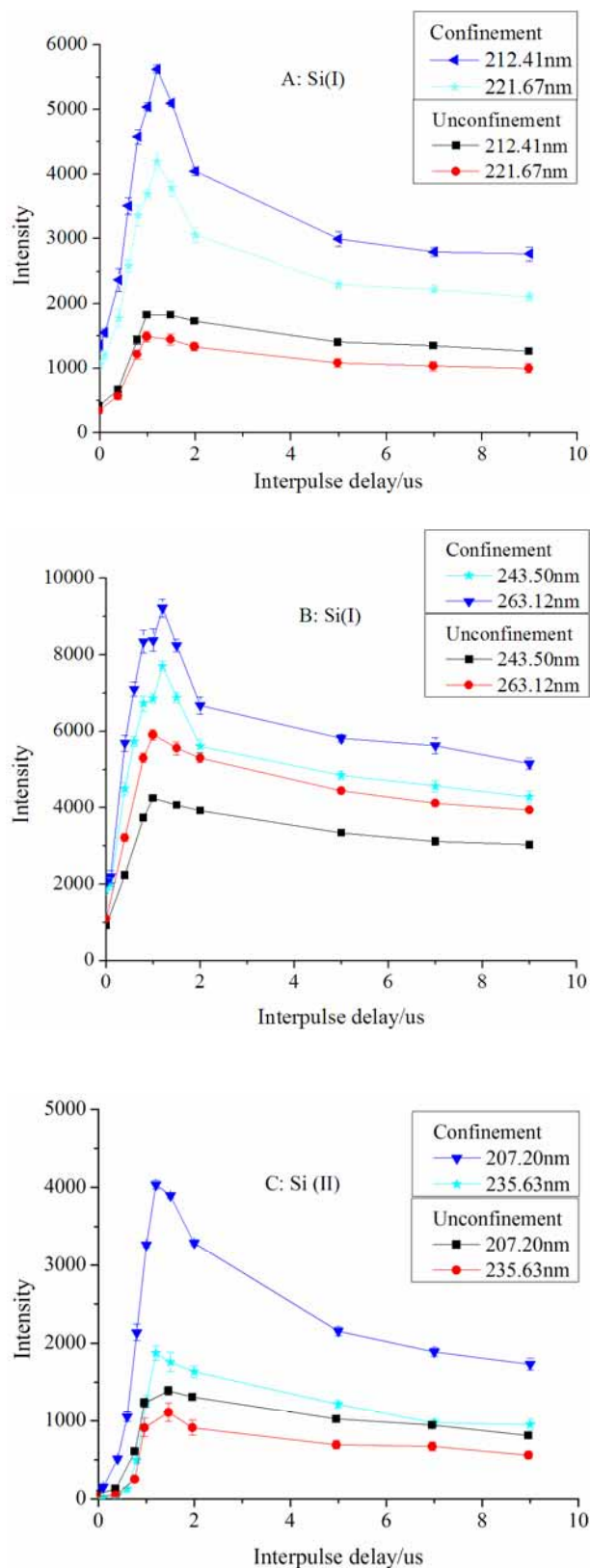


Fig.3. Pulse Time delay dependence of the emission intensities of several Si lines for dual pulse laser plasma with and without spatial confinement. ($E = 20\text{mJ} + 20\text{mJ}$, $t_d = 1.0 \mu\text{s}$)

It has also ascertained that the signal intensity from the confined collinear dual pulse excitation shows a

1
2
3
4 better stability. As shown in table 1, the relative standard deviation of all the selected lines with
5
6 confinement is lower than that without confinement. The RSD improve factor, which is defined as the
7
8 quotient of RSD of the confined DP-LIBS spectral line dividing by the RSD of the corresponding
9
10 unconfined DP-LIBS spectral line is listed in table 1 either. Typically, an improve factor of 2-4 is
11
12 obtained, dependent on the selected line. Recently, Wang et al. [18] reported that by using a cylindrical
13
14 cavity with height of 1.5 mm and diameter of 3 mm could effectively reduce the spectral signal RSD of
15
16 the laser plasma. However, in an previous study by Popov et al. [16], a higher RSD was observed
17
18 compared with the LIBS spectra when using a cylindrical cavity with height of 4 mm and diameter of 4
19
20 mm. In collinear dual pulse LIBS with cavity confinement, the result observed here indicating that the
21
22 cavity confinement can possibly be used to improve the signal repeatability as well, and therefore
23
24 improve the analytical capability of LIBS technique, although the effects might vary with different
25
26 cavity shapes and sizes, as observed by Wang and Popov.

27 28 **3.2. Temperature and electron number density**

29
30 Generally, the local thermodynamical equilibrium (LTE) is an appropriate description for the
31
32 laser-induced plasma, in both the double excitation and cavity confinement. Under LTE assumption,
33
34 electron temperature and electron number density can be estimated by means of spectroscopic
35
36 measurements, and the Boltzmann plot is then used to derive the electron temperature of the plasma.[26,
37
38 27] The line intensity was defined as the area of an emission line after Lorentz curve fitting. After
39
40 correcting the measured line intensities for the spectral response of the optical system, the relative
41
42 intensities of seven well isolated Si atomic lines (243.5 nm, 250.69 nm, 252.41 nm, 252.85nm,
43
44 263.13nm, 298.77 nm, 390.55 nm) were used to draw Boltzmann plots for both unconfined dual pulse
45
46 laser plasma (Figure 4a) and confined dual pulse laser plasma (Figure 4b), and the estimated electron
47
48 temperatures of unconfined collinear dual pulse laser plasma and confined collinear dual pulse laser
49
50 plasma were 11967 ± 523 K and 13859 ± 605 K, respectively. The uncertainty provided here was the
51
52 standard deviation of five repeated measurements. An increment of electron temperature was observed
53
54 in the confined collinear dual pulse laser plasma. Probably, As a result, more atoms and ions will be
55
56 excited to upper electronic states in the laser plasma with cavity confinement, in consistent with the
57
58 enhanced optical emission of confined laser plasma.
59
60

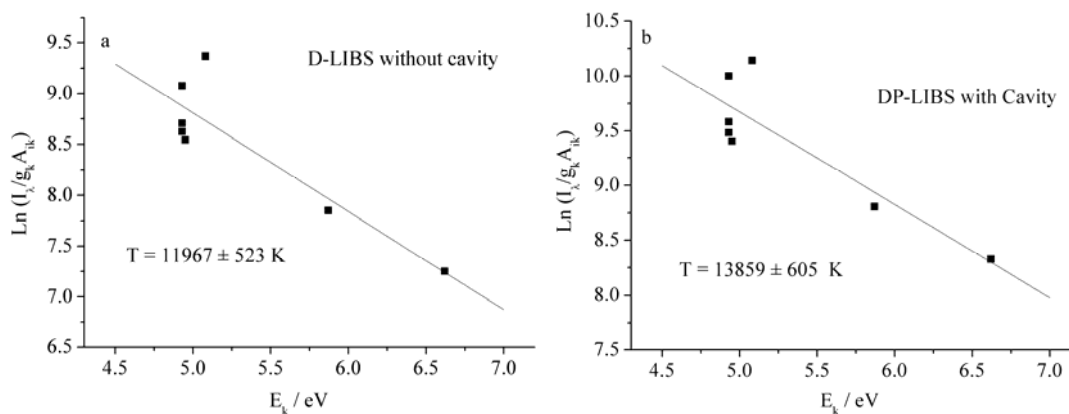


Figure 4. Boltzmann plot of Si lines from plasma of (a) unconfined collinear DP-LIBS and (b) confined collinear DP-LIBS. $E = 20\text{mJ} + 20\text{mJ}$, $\Delta t = 1.5 \mu\text{s}$, $t_d = 1.0 \mu\text{s}$

The experimental linewidth of the isolated Si I 212.41 nm line was used to estimate the electron number density here. Generally, the Stark broadening, Doppler broadening and pressure broadening will affect the observed linewidth in LIBS spectra at atmosphere. And the expected Doppler broadening can be easily estimated to be less than 0.004 nm for Si I 212.41 nm at a temperature of 10000 K. This represents a very small contribution to the total line width and can be safely neglected. The instrumental line width $\Delta\lambda_{ins}$ of the Avantes Spectrometer system has been found to be 0.1 nm[28]. And the Stark broadening is the primary mechanism influencing the linewidth of plasma emission spectra[27], which results from collisions of charged species. And the electron number density N_e in cm^{-3} related to Stark broadening lines is given by $\Delta\lambda_{1/2} = 2\omega \left(\frac{N_e}{10^{16}} \right)$. Where ω is the electron impact width parameter (nm), $\Delta\lambda_{1/2}$ is the half width half maximum (HWHM) of the Stark broadening linewidth of the considered transition line. It can be derived from the measured experimental linewidth by taking into account instrumental broadening and Doppler broadening.

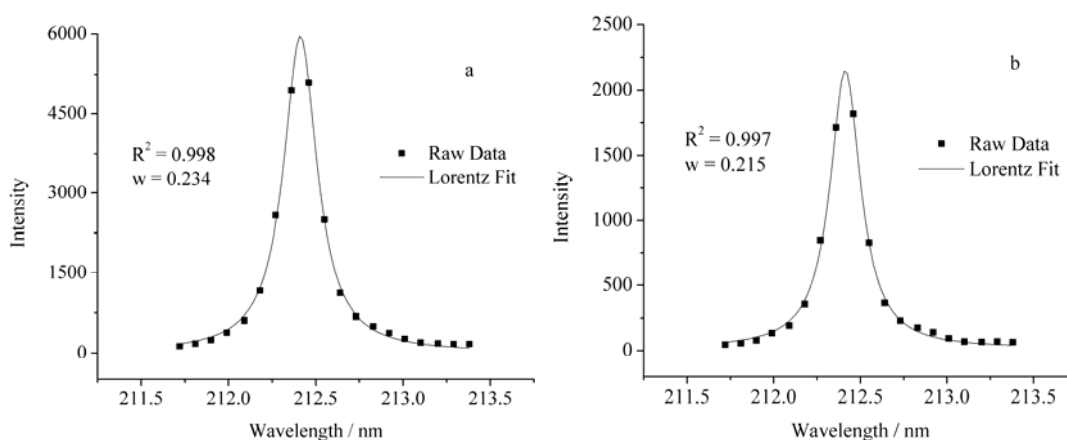


Figure 5. Si I 212.7 nm line profiles of optical emission in collinear dual pulse laser induced plasma (a) with and (b) without cavity confinement. ($E = 20\text{mJ} + 20\text{mJ}$, $\Delta t = 1.5 \mu\text{s}$, $t_d = 1.0 \mu\text{s}$)

1
2
3
4 The typical Lorentz fitting curves of the experimental line width $\Delta\lambda$ of the isolated Si lines 212.4 nm
5
6 in confined collinear DP-LIBS and unconfined collinear DP-LIBS are shown in Figure 5a and 5b
7
8 respectively, and the value in confined collinear DP-LIBS was slightly higher than that in unconfined
9
10 collinear DP-LIBS. After subtracting the effect of instrument broadening, the estimated electron
11
12 number density in confined and unconfined collinear dual pulse laser plasma were estimated to be
13
14 $(8.18 \pm 0.01) \times 10^{17} \text{ cm}^3$ and $(7.06 \pm 0.02) \times 10^{17} \text{ cm}^3$, respectively. Similar to that of
15
16 temperature, the electron number densities in the confined collinear dual pulse laser plasma are higher
17
18 than that in the unconfined laser plasma. Similarly, the standard deviation of five repeated
19
20 measurements was served as the uncertainty of measured electron number density. As a result, more
21
22 atoms and ions will be excited to upper electronic states in the cavity confined laser plasma, insistent
23
24 with the optical emission enhancement observed above.
25

26 27 **4 Conclusion**

28
29
30 The optical emission of cylindrical cavity confined collinear dual pulse laser induced plasma was
31
32 carefully studied and compared with the collinear dual pulse laser induced plasma without a cavity.
33
34 Obvious optical emission enhancement was observed along with an improved signal to noise ratio.
35
36 From the relative standard deviation of several selected Si lines, it has also ascertained that the signal
37
38 intensity from confined collinear dual pulse excitation showed a better stability. The optimized delay
39
40 time between two laser pulses to achieve the maximum atomic and ionic line intensity had also been
41
42 investigated. And a modest difference of the optimized inter-pulse delay time was found between
43
44 collinear DP-LIBS with and without cavity confinement. Seven silicon atomic line intensities were
45
46 measured and used to derived the electron temperature by employing the Boltzmann plots, while the
47
48 electron number density was determined by using the Stark broadening of Si I 212.41 nm linewidth.
49
50 Compared to the collinear dual laser induced plasma, both the temperature and electron number density
51
52 of the cavity confined plasma were increased, in consistent with the enhancement of optical emission.
53

54 55 **Acknowledgements**

56
57
58 This study was supported by the National Natural Science Foundation of China (Grant No. 61178034)
59
60 and the Natural Science Foundation of Zhejiang Province (LY14F050003), and partially supported by
the Program for Innovative Research Team, Zhejiang Normal University, China.

References

- [1] A. Cremers, L. Radziemski, Handbook of laser-induced breakdown spectroscopy, in, John Wiley & Sons, London, 2006.
- [2] J.P. Singh, S.N. Thakkur, Laser-Induced Breakdown Spectroscopy, Elsevier Science, Oxford, 2007.
- [3] Z. Wang, T. Yuan, Z. Hou, W. Zhou, J. Lu, H. Ding, X. Zeng, *Frontiers of Physics*, 8 (2013) 19.
- [4] B. Bousquet, J.-B. Sirven, L. Canioni, *Spectrochimica Acta Part B: Atomic Spectroscopy*, 62 (2007) 1582-1589.
- [5] L.J. Radziemski, D.A. Cremers, *Laser-Induced Plasmas and Applications*, in, Marcel Dekker, New York, 1989.
- [6] K.J. Grant, G.L. Paul, J.A. O'Neill, *Appl Spectrosc*, 45 (1991) 701-705.
- [7] D. Death, A. Cunningham, L. Pollard, *Spectrochimica Acta Part B: Atomic Spectroscopy*, 64 (2009) 1048-1058.
- [8] X. Li, W. Zhou, K. Li, H. Qian, Z. Ren, *Opt Commun*, 285 (2012) 54-58.
- [9] C. Gautier, P. Fichet, D. Menut, J.L. Lacour, D. L'Hermite, J. Dubessy, *Spectrochim Acta B*, 60 (2005) 792-804.
- [10] C. Gautier, P. Fichet, D. Menut, J.L. Lacour, D. L'Hermite, J. Dubessy, *Spectrochim Acta B*, 60 (2005) 265-276.
- [11] D.K. Killinger, S.D. Allen, R.D. Waterbury, C. Stefano, E.L. Dottery, *Optics Express*, 15 (2007) 12905-12915.
- [12] O.A. Nassef, H.E. Elsayed-Ali, *Spectrochim Acta B*, 60 (2005) 1564-1572.
- [13] K. Li, W. Zhou, Q. Shen, Z. Ren, B. Peng, *J Anal Atom Spectrom*, 25 (2010) 1475-1481.
- [14] W. Zhou, K. Li, H. Qian, Z. Ren, Y. Yu, *Applied Optics*, 51 (2012) B42-B48.
- [15] W. Zhou, K. Li, X. Li, H. Qian, J. Shao, X. Fang, P. Xie, W. Liu, *Opt Lett*, 36 (2011) 2961-2963.
- [16] A.M. Popov, F. Colao, R. Fantoni, *Journal of Analytical Atomic Spectrometry*, 24 (2009) 602-604.

- 1
2
3
4 [17] A.M. Popov, F. Colao, R. Fantoni, *Journal of Analytical Atomic Spectrometry*, 25 (2010) 837-848.
5
6
7 [18] L.B. Guo, C.M. Li, W. Hu, Y.S. Zhou, B.Y. Zhang, Z.X. Cai, X.Y. Zeng, Y.F. Lu, *Applied Physics Letters*, 98
8
9 (2011).
10
11 [19] Z. Wang, Z. Hou, S.-I. Lui, D. Jiang, J. Liu, Z. Li, *Optics Express*, 20 (2012) A1011-A1018.
12
13 [20] Z. Hou, Z. Wang, J. Liu, W. Ni, Z. Li, *Optics Express*, 21 (2013) 15974-15979.
14
15 [21] A. Kuwako, Y. Uchida, K. Maeda, *Applied optics*, 42 (2003) 6052-6056.
16
17
18 [22] L.B. Guo, B.Y. Zhang, X.N. He, C.M. Li, Y.S. Zhou, T. Wu, J.B. Park, X.Y. Zeng, Y.F. Lu, *Optics Express*, 20
19
20 (2012) 1436-1443.
21
22 [23] X. Zeng, X. Mao, S.S. Mao, J.H. Yoo, R. Greif, R.E. Russo, *Journal Applied Physics*, 95 (2004).
23
24 [24] L.B. Guo, W. Hu, B.Y. Zhang, X.N. He, C.M. Li, Y.S. Zhou, Z.X. Cai, X.Y. Zeng, Y.F. Lu, *Optics Express*, 19
25
26 (2011) 14067-14075.
27
28 [25] Z. Hou, Z. Wang, J. Liu, W. Ni, Z. Li, *Optics Express*, 22 (2014) 12909-12914.
29
30 [26] H.R. Griem, *Plasma Spectroscopy*, McGraw-Hill Inc., New York, 1964.
31
32 [27] H. Griem, *Principles of Plasma Spectroscopy*, Cambridge University Press, Cambridge, 1997.
33
34 [28] W. Zhou, X. Su, H. Qian, K. Li, X. Li, Y. Yu, Z. Ren, *J Anal Atom Spectrom*, 28 (2013) 702-710.
35
36
37
38
39
40
41
42
43
44
45
46
47
48
49
50
51
52
53
54
55
56
57
58
59
60